

## Aluminum beam reinforced by externally bonded composite materials

Rabahi Abderezak<sup>1,2</sup>, Tahar Hassaine Daouadji<sup>\*1,2</sup> and Benferhat Rabia<sup>1,2</sup>

<sup>1</sup> *Laboratory of Geomatics and Sustainable Development, University of Tiaret, Algeria*

<sup>2</sup> *Department of Civil Engineering, Ibn Khaldoun University of Tiaret, Algeria*

(Received August 10, 2020, Revised December 10, 2020, Accepted December 18, 2020)

**Abstract.** A recently popular method for retrofitting reinforced structure beams is to bond composite plates to their tensile faces. An important failure mode of such plated beams is the debonding of the composite plates from the base material of the beam due to high level of stress concentration in the adhesive at the ends of the composite plate. This paper, shows and presents in more detail a closed-form rigorous solution for interfacial stress in cantilever aluminum beams strengthened with bonded composite (sika wrap) plates and subjected to a uniformly distributed load. The results show that there exists a high concentration of both shear and normal stress at the ends of the laminate, which might result in premature failure of the strengthening scheme at these locations. A parametric study has been conducted to investigate the sensitivity of interface behavior to parameters such as laminate and adhesive stiffness, the thickness of the laminate; the effect on plate length of the strengthened cantilever beam region, the effect of adhesive (modules, thickness) and the effect of loading and geometry for the cantilever beam; where all were found to have a marked effect on the magnitude of maximum shear and normal stress in the composite member. The theoretical predictions are compared with other existing solutions. Finally, this research is helpful for the understanding on mechanical behaviour of the interface and design of the composite-aluminum hybrid structures.

**Keywords:** strengthening; shear lag effect; sika wrap composite plate; interfacial stresses; aluminum cantilever beam

### 1. Introduction

In recent applications, the use of laminates has been explored both in laboratory tests (Abderezak *et al.* 2019, Hamrat *et al.* 2020, Daouadji 2013, Abdelouahed 2006 and Yuan *et al.* 2019 and Tayeb *et al.* 2020) and in field applications on bridges (Chaded *et al.* 2018, Rabia *et al.* 2018, Tayeb and Daouadji 2020, Daouadji 2016b and Guenaneche and Tounsi 2014) and other types of structure (Amara *et al.* 2019, Liu *et al.* 2019, Panjehpour *et al.* 2016, Larrinaga *et al.* 2020, Daouadji 2017, Tounsi *et al.* 2008, Wang *et al.* 2020, Smith and Teng 2002). Using laminate composite for reinforcement of beams, the ultra high tensile strength of the composite material can be better utilized, which gives a more effective strengthening scheme. In steel structures (like metal), compressive stresses introduced to the tension flange of a steel beam, for instance, will improve fatigue resistance of the steel beam (Tahar *et al.* 2019, Rabia *et al.* 2019, Bensattalah *et al.* 2016,

---

\*Corresponding author, Professor, E-mail: daouadjitahar@gmail.com

Benachour *et al.* 2008 and Bouakaz *et al.* 2014). Furthermore, the strengthening effect obtained when laminates are employed will not only be limited to additional imposed loads on the strengthened structure, but will also participate in carrying a portion of the dead load. Analysis of interfacial stress in beams with bonded plates has been performed by several researchers. The analyses provided closed-form formulas for the calculation of interfacial shear and peeling stress in beams with bonded plates or laminates.

The most common failure mode for FRP-strengthened beams is debonding of the composite plate. This premature mode is caused by interfacial stress concentration in the adhesive layer. In the literature, we have found that there is not much study of the concentration of interfacial stresses in aluminum beams reinforced with composite laminates (Tahar *et al.* 2020, Khelifa *et al.* 2018, Bensattalah *et al.* 2018, Belabed *et al.* 2018, Chergui *et al.* 2019, Rabahi *et al.* 2016, Sahla *et al.* 2019, Matouk *et al.* 2020, Daouadji and Benferhat 2016, Tounsi *et al.* 2013, Benhenni *et al.* 2019b, Menasria *et al.* 2020, Mokhtar *et al.* 2018, Rabhi *et al.* 2020, Daouadji and Adim 2016a, Rahmani *et al.* 2020 and Benferhat *et al.* 2016). To the knowledge of the authors, very few theoretical results that have been published on interfacial stress concentration in aluminum beams reinforced with bonded laminates considering the current bending load cases. For that we the authors; we thought to present this research, which deals with the case of a aluminum beam strengthened with composite plate. Closed-form solutions of such stresses are thus required in developing design guidelines for strengthening aluminum beams with bonded laminated plates. The present model is general in nature, and it is applicable to more general loads cases. With the escalating use of this strengthening scheme, there is a great need for calculation models that can be used to predict the magnitude of maximum interfacial shear stress at the end of the laminate. There is also some lack of knowledge today regarding how material and geometric properties of the strengthening system (composite materials and adhesive) should be chosen in order to minimize the magnitude of these interfacial stresses and ensure sufficient strength of the strengthening system without need for expensive and complicated mechanical anchorage devices.

In this paper, a general new solution is developed to predict both shear and normal interfacial stress in aluminum cantilever beams strengthened with bonded sika wrap composite laminates, the considered beam is subjected to a uniformly distributed load. Hence, compared with the existing solutions such as presented by Hue Ju He model (2019), the present model is general in nature, and it is applicable to more general loads cases. With the escalating use of this strengthening scheme, there is a great need for calculation models that can be used to predict the magnitude of maximum interfacial stress at the end of the laminate. There is also some lack of knowledge today regarding how material and geometric properties of the strengthening system (base material of the beam, composite materials and adhesive) should be chosen in order to minimize the magnitude of these interfacial stresses and ensure sufficient strength of the strengthening of the system without need for expensive and complicated mechanical anchorage devices.

We can also mention, in addition to the composite fiber matrix materials, another alternative can be proposed to strengthen the aluminum structures that will be addressed in our future research, it is therefore the use of functionally graded materials FGM (Abderezak *et al.* 2016, 2018, Belkacem *et al.* 2018, Abualnour *et al.* 2018, Al-Furjan *et al.* 2020a, Addou *et al.* 2019, Al-Furjan *et al.* 2020a, Alimirzaei *et al.* 2019, Balubaid *et al.* 2019, Boukhelif *et al.* 2019, Boulefrakh *et al.* 2019, Berghouti *et al.* 2019, Bourada *et al.* 2019, Abderezak *et al.* 2020, Refrafi *et al.* 2020, Shariati *et al.* 2020, Bourada *et al.* 2020, Bousahla *et al.* 2020, Bellal *et al.* 2020, Benferhat *et al.* 2016a and Benhenni *et al.* 2019a), that in order to improve and ensure the material continuity through the thickness of the reinforcing plate, aiming as a parameter in the mechanical characteristics of FGM, all by passing

laws adequately mixes to better meet industrial requirements and the environmental condition.

## 2. The method of solution

### 2.1 Study and analysis

The most common failure modes for composite strengthened cantilever beams are debonding of the composite plate. These types of failures prevent the strengthened cantilever beam for reaching its ultimate flexural capacity, and therefore they must be included in design considerations. Both of these premature failure modes are caused by shear and normal stress concentrations in adhesive layer. Closed form solutions of stress concentrations are required in developing design guidelines for strengthening reinforced aluminum cantilever beams with sika wrap composite plates. In the present analysis takes into consideration the transverse shear stress and strain in the cantilever aluminum beam and the plate but ignores the transverse normal stress in them. One of the analytical approaches proposed by Tahar *et al.* (2019) for steel beam strengthened with a bonded composite plate (Fig. 1) was used in order to compare it with other analytical solutions.

The analytical approach is based on the following assumptions (Tahar *et al.* 2019):

- (1) Elastic stress strain relationship for aluminum cantilever beam, composite plate and adhesive;
- (2) There is a perfect bond between the composite plate and the aluminum cantilever beam;
- (3) The adhesive is assumed to only play a role in transferring the stresses from the aluminum cantilever beam to the composite plate reinforcement;
- (4) The stresses in the adhesive layer do not change through the direction of the thickness;

Since the composite laminate is an orthotropic material, its material properties vary from layer to layer. In theoretical study (Tahar *et al.* 2019), the laminate theory is used to determine the stress and strain behaviours of the externally bonded composite plate in order to investigate the whole mechanical performance of the composite – strengthened structure. The laminate theory is used to determine the stress and strain of the externally bonded composite plate in order to investigate the whole mechanical performance of the composite strengthened structure. The effective modules of the composite laminate are varied by the orientation of the fibre directions and arrangements of

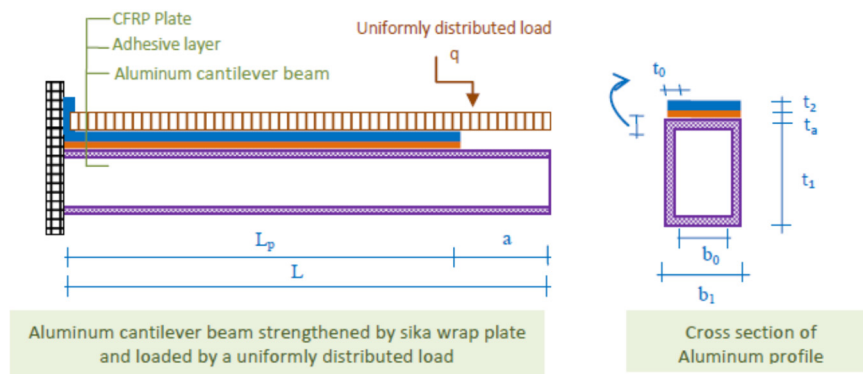


Fig. 1 Structure configuration of a aluminum cantilever beam strengthened by Sika wrap plate

the laminate patterns. The classical laminate theory is used to estimate the strain of the composite plate, i.e.

$$\begin{Bmatrix} \varepsilon^0 \\ k \end{Bmatrix} = \begin{bmatrix} A' & B' \\ C' & D' \end{bmatrix} \begin{Bmatrix} N \\ M \end{Bmatrix} \quad (1)$$

$$\begin{aligned} [A'] &= [A]^{-1} + [A]^{-1}[B][D^*]^{-1}[B][A]^{-1} \\ [B'] &= -[A]^{-1}[B][D^*]^{-1} \\ [C'] &= [B']^T \\ [D'] &= [D^*]^{-1} \\ [D^*] &= [D] - [B][A]^{-1}[B] \end{aligned} \quad (2)$$

The terms of the matrices  $[A]$ ,  $[B]$  and  $[D]$  are written as

Extensional matrix

$$A_{ij} = \sum_{k=1}^{nl} \bar{Q}_{ij}^k ((y_2)_k - (y_2)_{k-1}) \quad (3)$$

Extensional –bending coupled matrix

$$B_{ij} = \frac{1}{2} \sum_{k=1}^{nl} \bar{Q}_{ij}^k ((y_2^2)_k - (y_2^2)_{k-1}) \quad (4)$$

Flexural matrix

$$D_{ij} = \frac{1}{3} \sum_{k=1}^{nl} \bar{Q}_{ij}^k ((y_2^3)_k - (y_2^3)_{k-1}) \quad (5)$$

The subscript 'nl' represents the number of laminate layers of the FRP plate,  $\bar{Q}_{ij}$  can be estimated by using the off-axis orthotropic plate theory, where

$$\bar{Q}_{11} = Q_{11}m^4 + 2(Q_{12} + 2Q_{33})m^2n^2 + Q_{22}n^4 \quad (6)$$

$$\bar{Q}_{12} = (Q_{11} + Q_{22} - 4Q_{33})m^2n^2 + Q_{12}(n^4 + m^4) \quad (7)$$

$$\bar{Q}_{22} = Q_{11}n^4 + 2(Q_{12} + 2Q_{33})m^2n^2 + Q_{22}m^4 \quad (8)$$

$$\bar{Q}_{33} = (Q_{11} + Q_{22} - 2Q_{12} - 2Q_{33})m^2n^2 + Q_{33}(n^4 + m^4) \quad (9)$$

And

$$\begin{aligned} Q_{11} &= \frac{E_1}{1 - \nu_{12}\nu_{21}}, & Q_{22} &= \frac{E_2}{1 - \nu_{12}\nu_{21}}, & Q_{12} &= \frac{\nu_{12}E_2}{1 - \nu_{12}\nu_{21}} = \frac{\nu_{21}E_1}{1 - \nu_{12}\nu_{21}}, \\ Q_{33} &= G_{12}, & m &= \cos(\theta_j), & n &= \sin(\theta_j) \end{aligned} \quad (10)$$

Where  $j$  is number of the layer;  $h$ ,  $\bar{Q}_{ij}$  and  $\theta_j$  are respectively the thickness, the Hooke's elastic

tensor and the fibers orientation of each layer.

**Mathematical formulation of the present method:**

A differential section  $dx$ , can be cut out from the composite reinforced aluminum cantilever beam as shown in Fig. 2. The composite beam is made from three materials: the aluminum, adhesive layer and composite reinforcement. In the present analysis, all of the materials are assumed to display linear elastic behaviour; the adhesive is assumed to play a role only in transferring the stresses from the aluminum to the sika wrap reinforcement and the stresses in the adhesive layer do not change through the direction of the thickness.

The longitudinal resultant forces,  $N_1$  and  $N_2$ , for the lower adherends is

$$N_1 = b_1 \int_0^{t_1} \sigma_1^N(y) dy \tag{11}$$

Where  $\sigma_1^N$  is longitudinal normal stresses for the lower adherends, and which can be rewritten in the form

$$N_1 = E_1 b_1 \int_0^{t_1} \frac{dU_1^N}{dx} dy = E_1 A_1 \left( \frac{du_1^N}{dx} - \frac{t_1}{4G_1} \frac{d\tau_a}{dx} \right) \tag{12}$$

The deformation in concrete in the vicinity of the adhesive layer can be expressed by

$$\varepsilon_1(x) = \frac{du_1(x)}{dx} = \varepsilon_1^M(x) + \varepsilon_1^N(x) \tag{13}$$

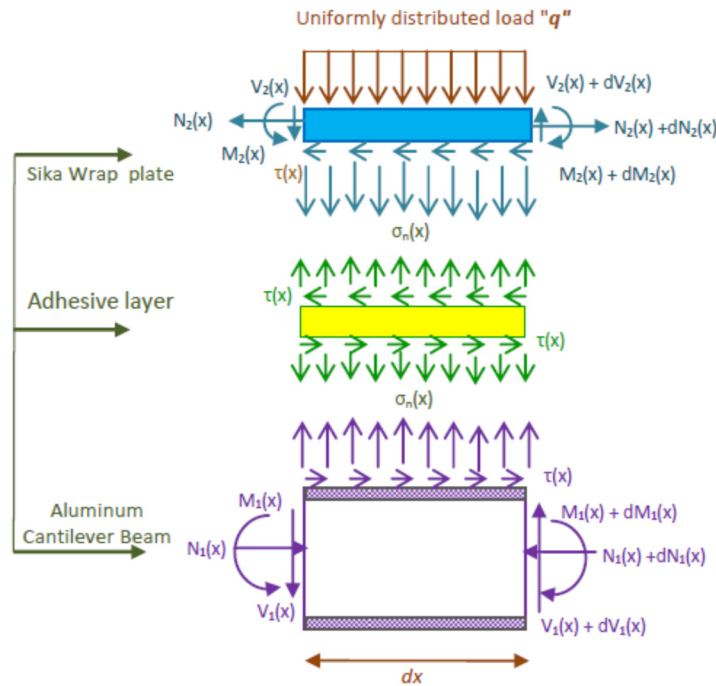


Fig. 2 Forces in infinitesimal element of a soffit- Sika wrap plated aluminum cantilever beam

with

$$\varepsilon_1^M(x) = \frac{y_1}{E_1 I_1} M_1(x) \quad (14)$$

$$\varepsilon_1^N(x) = \frac{du_1^N(x)}{dx} = \frac{N_1}{E_1 A_1} + \frac{t_1}{4G_1} \frac{d\tau_a}{dx} \quad (15)$$

$$\varepsilon_1(x) = \frac{du_1(x)}{dx} = \frac{y_1}{E_1 I_1} M_1(x) + \frac{N_1(x)}{E_1 A_1} + \frac{t_1}{4G_1} \frac{d\tau_a}{dx} \quad (16)$$

The longitudinal resultant force  $N_2$  for the upper adherends is

$$N_2 = b_2 \int_0^{t_2} \sigma_2^N(y') dy' \quad (17)$$

Where  $\sigma_2^N$  is longitudinal normal stresses for the upper adherends, and which can be rewritten in the form

$$N_2 = E_2 b_2 \int_0^{t_2} \frac{dU_2^N}{dx} dy' = E_2 A_2 \left( \frac{du_2^N}{dx} + \frac{5t_2}{12G_2} \frac{d\tau_a}{dx} \right) \quad (18)$$

Based on the theory of laminated sheets, the deformation of the composite sheet in the vicinity of the adhesive layer is given by

$$\varepsilon_2(x) = \frac{du_2(x)}{dx} = \varepsilon_2^M(x) + \varepsilon_2^N(x) \quad (19)$$

with

$$\varepsilon_2^M(x) = \frac{-y_2}{E_2 I_2} M_2(x) \quad (20)$$

$$\varepsilon_2^N(x) = \frac{du_2^N(x)}{dx} = A_{11} \frac{N_2(x)}{b_2} - \frac{5t_2}{12G_2} \frac{d\tau_a}{dx} \quad (21)$$

$$\varepsilon_2(x) = \frac{du_2(x)}{dx} = -D_{11} \frac{y_2}{b_2} M_2(x) + A_{11} \frac{N_2(x)}{b_2} - \frac{5t_2}{12G_2} \frac{d\tau_a}{dx} \quad (22)$$

Where  $u_1(x)$  and  $u_2(x)$  are the horizontal displacements of the aluminum cantilever beam and the sika wrap composite plate respectively.  $M_1(x)$  and  $M_2(x)$  are respectively the bending moments applied to the aluminum beam and the composite plate;  $E_1$  is the Young's modulus of aluminum;  $I_1$  the moment of inertia,  $N_1$  and  $N_2$  are the axial forces applied to the aluminum and the composite plate respectively,  $b_1$  and  $t_1$  are the width and thickness of the reinforcement plate,  $[A'] = [A^{-1}]$  is the inverse of the membrane matrix  $[A]$ ,  $[D'] = [D^{-1}]$  is the inverse of the bending matrix.

By writing the conditions of equilibrium of the member 1 (Aluminum), we will have:

In the  $x$  direction:

$$\frac{dN_1(x)}{dx} = -b_1 \tau(x) \quad (23)$$

Where  $\tau(x)$  is the shear stress in the adhesive layer.

In the  $y$  direction:

$$\frac{dV_1(x)}{dx} = -(\sigma_n(x)b_1 + qb_1) \quad (24)$$

Where  $V_1(x)$  the sheer force of the concrete beam is,  $\sigma(x)$  is the normal stress at the adhesive layer,  $q$  is the distributed load and  $b_1$  the width of the aluminum beam.

The moment of balance:

$$\frac{dM_1(x)}{dx} = V_1(x) - b_1y_1\tau(x) \quad (25)$$

The balance of the sika wrap reinforcement plate in the  $x$  and  $y$  directions, as well as the moment of equilibrium are written as follows:

In the  $x$  direction:

$$\frac{dN_2(x)}{dx} = b_2\tau(x) \quad (26)$$

In the  $y$  direction:

$$\frac{dV_2(x)}{dx} = \sigma_n(x)b_2 \quad (27)$$

The moment of balance:

$$\frac{dM_2(x)}{dx} = V_2(x) - b_2y_2\tau(x) \quad (28)$$

Where  $V_2(x)$  is the shear force of the reinforcement plate.

In what follows, the stiffness of the reinforcement plate is significantly lower than that of the aluminum beam to be reinforced. The bending moment in the composite plate can be neglected to simplify the shear stress derivation operations.

## 2.2 Shear stress distribution along the Sika wrap–aluminum interface

The governing differential equation for the interfacial shear stress is expressed as (Tahar *et al.* 2019)

$$\begin{aligned} \frac{d^2\tau(x)}{dx^2} - \frac{3G_1G_a}{3G_1t_a + \phi G_a t_1} \left( \frac{E_1A_1A'_{11} + b_2}{E_1A_1} + \frac{(t_1 + t_2)(t_1 + t_2 + 2t_a)b_2D'_{11}}{2E_1I_1D'_{11} + b_2} \right) \tau(x) \\ + \frac{3G_1G_a(t_1 + t_2)D'_{11}}{(6G_1t_a + 2\phi G_a t_1)(E_1I_1D'_{11} + b_2)} V_T(x) = 0 \end{aligned} \quad (29)$$

Where  $\phi$  is a geometrical coefficient which is given as

$$\phi = \frac{1}{2A_1t_1^2} [b_1(-t_0^3 + 6t_0t_1^2 - t_1^3 + (t_1 - t_0)^3) + b_0(3t_1^2(t_1 - 2t_0) - (t_1 - t_0)^3 + t_0^3)] \quad (30)$$

For a rectangular section ( $b_1 = b_0$ ),  $\phi = 1$  which corresponds to the same expression given by Tahar *et al.* (2019). However, for aluminum beam section we have  $\phi < 1$ . For simplicity, the general solutions presented below are limited to loading which is either concentrated or uniformly distributed over part or the whole span of the beam, or both (Fig. 1). For such loading,  $d^2V_T(x)/dx^2 = 0$ , and the general solution to Eq. (29) is given by

$$\tau(x) = \mu_1 \cosh(\Delta x) + \mu_2 \sinh(\Delta x) + \frac{3G_a G_1 (2t_1 + t_2) D_{11}'}{4\Delta^2 (2G_1 t_a + \phi t_1 G_a) (E_1 I_1 D_{11}' + b_2)} V_T(x) \quad (31)$$

where  $\Delta$  is given as

$$\Delta = \sqrt{\frac{3G_1 G_a}{3G_1 t_a + \phi G_a t_1} \left( \frac{E_1 A_1 A_{11}' + b_2}{E_1 A_1} + \frac{(t_1 + t_2)(t_1 + t_2 + 2t_a) b_2 D_{11}'}{2E_1 I_1 D_{11}' + b_2} \right)} \quad (32)$$

and  $\mu_1$  and  $\mu_2$  are constant coefficients determined from the boundary conditions. In the present study, aluminum beam has been investigated which is subjected to a uniformly distributed load. The interfacial shear stress for this uniformly distributed load at any point is written as (Tahar *et al.* 2019)

$$\begin{aligned} \tau(x) = & \left( \frac{t_1 a (L - a)}{2E_1 I_1 \left( \frac{t_a}{G_a} + \frac{t_1}{3G_1} \phi \right)} - \frac{(t_1 + t_2) D_{11}'}{2\Delta^2 (E_1 I_1 D_{11}' + b_2)} \right) \frac{q e^{-\Delta x}}{\Delta} \\ & + \frac{t_1 + t_2}{2\Delta^2 (E_1 I_1 D_{11}' + b_2)} D_{11}' q \left( \frac{L}{2} - a - x \right) \end{aligned} \quad (33)$$

Where  $q$  is the uniformly distributed load and  $x$ ;  $a$ ;  $L$  and  $L_p$  are defined in Fig. 1.

### 2.3 Normal stress distribution along the Sika wrap–aluminum interface

The following governing differential equation for the interfacial normal stress (Tahar *et al.* 2019)

$$\frac{d^4 \sigma_n(x)}{dx^4} + \frac{E_a}{t_a} \left( D_{11}' + \frac{b_2}{E_1 I_1} \right) \sigma_n(x) - \frac{E_a}{t_a} \left( D_{11}' \frac{t_2}{2} - \frac{t_1 b_2}{2E_1 I_1} \right) \frac{d\tau(x)}{dx} + \frac{q E_a}{t_a E_1 I_1} = 0 \quad (34)$$

The general solution to this fourth–order differential equation is

$$\begin{aligned} \sigma_n(x) = & e^{-\chi x} [\mu_3 \cos(\chi x) + \mu_4 \sin(\chi x)] + e^{\chi x} [\mu_5 \cos(\chi x) + \mu_6 \sin(\chi x)] \\ & - \frac{2y_1 b_2 - (D_{11}' E_1 I_1 t_2)}{2(D_{11}' E_1 I_1 + b_2)} \frac{d\tau(x)}{dx} - \frac{q}{D_{11}' E_1 I_1 + b_2} \end{aligned} \quad (35)$$

For large values of  $x$  it is assumed that the normal stress approaches zero and, as a result,  $\mu_5 = \mu_6 = 0$ . The general solution therefore becomes

$$\sigma_n(x) = e^{-\chi x} [\mu_3 \cos(\chi x) + \mu_4 \sin(\chi x)] - \frac{2y_1 b_2 - (D_{11}' E_1 I_1 t_2)}{2(D_{11}' E_1 I_1 + b_2)} \frac{d\tau(x)}{dx} - \frac{q}{D_{11}' E_1 I_1 + b_2} \quad (36)$$



Where

$$\chi = \sqrt[4]{\frac{E_a}{4t_a} \left( D_{11}' + \frac{b_2}{E_1 I_1} \right)} \quad (37)$$

As is described by Hassaine Daouadji (Tahar *et al.* 2019), the constants  $\mu_3$  and  $\mu_4$  in Eq. (34) are determined using the appropriate boundary conditions and they are written as follows

$$\mu_3 = \frac{E_a}{2\chi^3 t_a E_1 I_1} [V_T(0) + \chi M_T(0)] - \frac{\lambda}{2\chi^3} \tau(0) + \frac{\rho}{2\chi^3} \left( \frac{d^4 \tau(0)}{dx^4} + \chi \frac{d^3 \tau(0)}{dx^3} \right) \quad (38)$$

$$\mu_4 = -\frac{E_a}{2\chi^2 t_a E_1 I_1} M_T(0) - \frac{2y_1 b_2 - (D_{11}' E_1 I_1 t_2)}{4\chi^2 (D_{11}' E_1 I_1 + b_2)} \frac{d^3 \tau(0)}{dx^3} \quad (39)$$

$$\rho = \frac{2y_1 b_2 - (D_{11}' E_1 I_1 t_2)}{2(D_{11}' E_1 I_1 + b_2)} \quad (40)$$

$$\lambda = \frac{E_a b_2}{t_a} \left( \frac{y_1}{E_1 I_1} - \frac{D_{11}' t_2}{2b_2} \right) \quad (41)$$

The above expressions for the constants  $\mu_3$  and  $\mu_4$  has been left in terms of the bending moment  $M_T(0)$  and shear force  $V_T(0)$  at the end of the soffit plate. With the constants  $\mu_3$  and  $\mu_4$  determined, the interfacial normal stress can then be found using Eq. (34).

### 3. Results and discussion

#### 3.1 Material used

A computer code based on the preceding equations was written to compute the interfacial stresses in a aluminum cantilever beam bonded with a sika wrap plate. The composite material was selected in the present examples as a bonded plate. However, the analysis is equally applicable to other types of composite material. The material used for the present studies is an aluminum cantilever beam bonded with composite plate. The cantilever beam is subjected to a uniformly distributed load ( $q = 15$  kN/ml). A summary of the geometric and material properties is given in Table 1 and Fig. 3 illustrates the dimensions of this aluminum cantilever beam.

Table 1 Geometric and mechanical properties of the materials used

Component	Width (mm)	Depth (mm)	Young's modulus (MPa)	Poisson's ratio
Adhesive layer	$b_a = 100$	$t_a = 2$	$E_a = 3000$	0.35
Aluminum plate	$b_2 = 100$	$t_2 = 4$	$E_2 = 65300$	0.3
Sika Wrap plate	$b_2 = 100$	$t_2 = 0,48$	$E_2 = 230\ 000$	0.28
Aluminum beam	$b_1 = 100$	$t_1 = 200$	$E_2 = 65300$	0.3

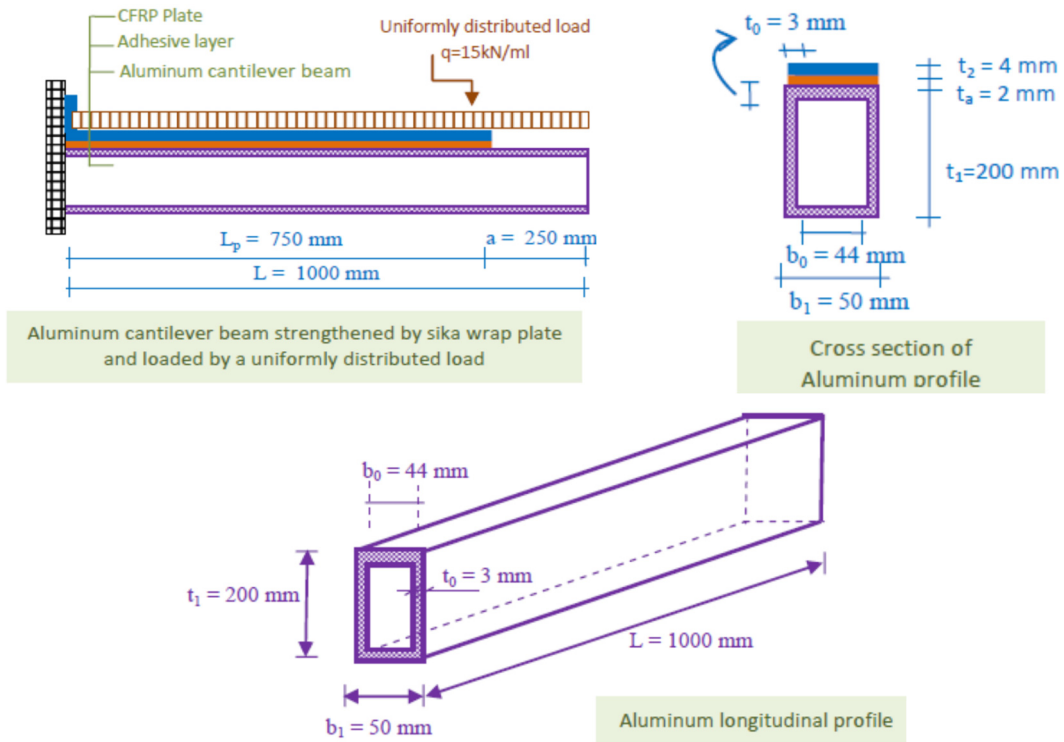


Fig. 3 Aluminum cantilever beam strengthened by Sika wrap plate: Geometric characteristic

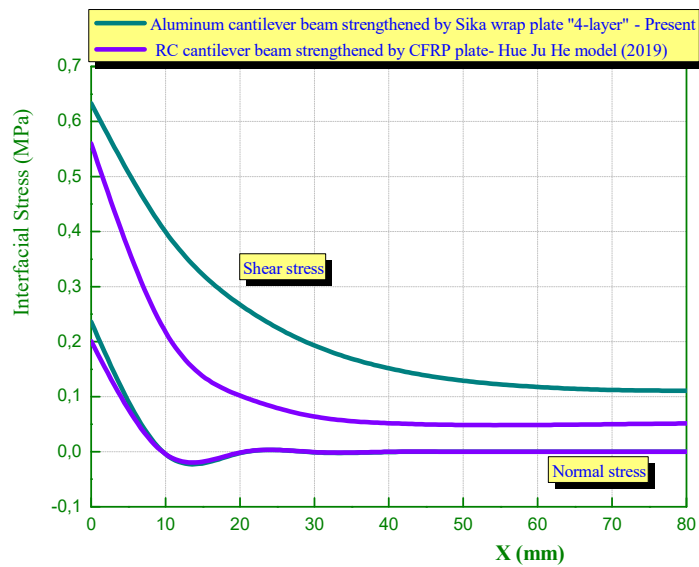


Fig. 4 Comparison of interfacial stress for Sika wrap plated Aluminum cantilever beam with the analytical results

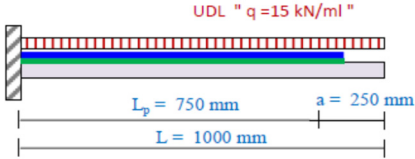
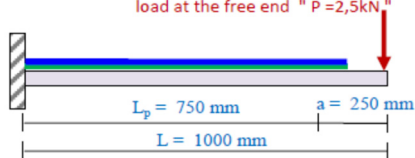
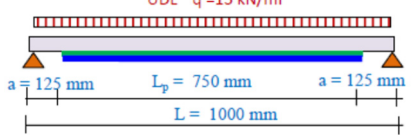
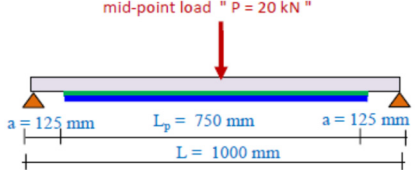
### 3.2 Comparison of predictions with existing solutions

The predicted stresses by the present theory have been compared to those of analytical results obtained by Hue Ju He model (2019). The geometry and materials properties of the specimen are summarized in Table 1 and Fig. 3. As it can be seen from Fig. 4 the predicted theoretical results agree with the analytical model results presented by Hue Ju He model (2019). Fig. 4 plots the interfacial shear and normal stresses near the plate end for the example aluminum cantilever beam bonded with a sika wrap plate for the uniformly distributed load case. Overall, the predictions of the different solutions agree closely with each other. The interfacial normal stress is seen to change sign at a short distance away from the plate end.

### 3.3 Effect of loading and geometry for the cantilever beam

Following the analysis of the results obtained (Table 2), while varying: the geometry of the beam (i.e., from a cantilever beam to a beam on two simple supports), the loading mode (from the uniformly distributed load to the concentrated load), also we varied the reinforcement plate from

Table 2 Comparison of interfacial stresses for a hybrid aluminum cantilever beam

Configuration of the beam (geometry and loading)	Comparison of interfacial stresses for a hybrid aluminum cantilever beam			
	Strengthened by sika wrap plate "4-layer"		Strengthened by aluminum plate "t <sub>2</sub> = 4 mm"	
	$\tau(x)$ (MPa)	$\sigma(x)$ (MPa)	$\tau(x)$ (MPa)	$\sigma(x)$ (MPa)
 <p>UDL "q =15 kN/ml "</p> <p><math>L_p = 750 \text{ mm}</math>    <math>a = 250 \text{ mm}</math> <math>L = 1000 \text{ mm}</math></p>	0.6331	0.2363	0.9315	0.8019
 <p>load at the free end " P =2,5kN "</p> <p><math>L_p = 750 \text{ mm}</math>    <math>a = 250 \text{ mm}</math> <math>L = 1000 \text{ mm}</math></p>	0.7839	0.2921	1.1182	0.9587
 <p>UDL "q =15 kN/ml "</p> <p><math>a = 125 \text{ mm}</math>    <math>L_p = 750 \text{ mm}</math>    <math>a = 125 \text{ mm}</math> <math>L = 1000 \text{ mm}</math></p>	1.0767	0.4015	1.5548	1.3354
 <p>mid-point load " P = 20 kN "</p> <p><math>a = 125 \text{ mm}</math>    <math>L_p = 750 \text{ mm}</math>    <math>a = 125 \text{ mm}</math> <math>L = 1000 \text{ mm}</math></p>	1.3577	0.5042	1.6882	1.4263

the sika wrap to the aluminum plate. We recorded very logical results, the fact that the thickness of the aluminum plate is greater than that of the sika wrap, the stresses become as important, the same for the geometry of the beam where the stress of a beam on two greater supports compared to a cantilever beam this is explained by the effect of the rigidity (since the system is hyper static) of the beam element.

### 3.4 Efficiency of strengthening cantilever aluminum beam by composite

Strain compatibility approach was used to predict the ultimate carrying capacity of the beams. A linear stress-strain curve for aluminum and sika wrap was taken into consideration in the study, the

Table 3 Comparison of Load-deflection for aluminum cantilever beam strengthened by sika wrap plate

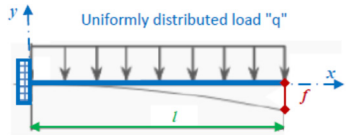
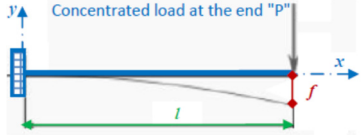
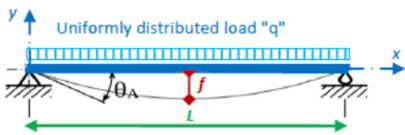
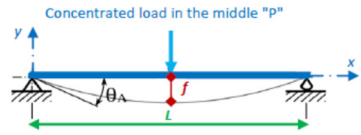
Aluminum cantilever beam L = 1000 mm	Load-deflection			
				
	Deflection (mm) for a $q = 15$ kN/ml	Maximum load $q_{\max}$ without deflection	Deflection (mm) for a $P = 20$ kN	Maximum load $P_{\max}$ without deflection
Aluminum cantilever beam "without strengthening"	$f = 1,36$ mm	$q_{\max} = 55,55$ kN/ml	$f = 4,84$ mm	$P_{\max} = 20,83$ kN
Aluminum cantilever beam strengthened by sika wrap plate "4-layer"	$f = 1,306$ mm	$q_{\max} = 57,47$ kN/ml	$f = 4,64$ mm	$P_{\max} = 21,74$ kN

Table 4 Comparison of Load-deflection for aluminum beam strengthened by sika wrap plate

Aluminum cantilever beam L = 2000 mm	Load-deflection			
				
	Deflection (mm) for a $q = 15$ kN/ml	Maximum load $q_{\max}$ without deflection	Deflection (mm) for a $P = 20$ kN	Maximum load $P_{\max}$ without deflection
Aluminum beam without strengthening	$f = 2,27$ mm	$q_{\max} = 33,33$ kN/ml	$f = 2,43$ mm	$P_{\max} = 41,66$ kN
Aluminum beam strengthened by sika wrap plate "4-layer"	$f = 2,18$ mm	$q_{\max} = 34,48$ kN/ml	$f = 2,32$ mm	$P_{\max} = 43,10$ kN

results of which are presented in Tables 3 and 4 (Load-deflection). Linear elastic behaviour of the sika wrap laminates was assumed based on the data provided by the manufacturer. Deflection of the beam was calculated using integration of the curvature along the span of each beam. Tables 3 and 4 shows a good correlation between the measured and predicted deflection of the beams. The results clearly show the interest of the reinforcement in comparison with a reinforced beam compared to a control beam (without reinforcement) or the deformation of this last side is important to that of the reinforced beam (whatever the geometry and the mode of loading), on the other hand the reinforced beam supports more load, and this is what is desired as a technical-economic solution, consequently the objective is achieved.

In conclusion, the use of sika wrap laminates to reinforce aluminum cantilever beams is an effective method to increase its ultimate load capacity and the behavior of most of the reinforced beams, was accompanied by a significant improvement in rigidity.

### 3.5 Effect of FRP plate thickness

The effect of plate stiffness “number of layers”, on interfacial normal stresses in strengthened aluminum cantilever beam, where the peak shear and peeling stresses for various thicknesses of the sika wrap strip appear in Figs. 5, 6 and 7. Of which we have presented in this study the effect of variation in the number of layers of sika wrap (in other words variation in the thickness of the composite plate), by way of example 2 layers, 4 layers, 6 layers, 8 layers and 10 layers. The thickness of the sika wrap plate is an important design variable in practice. The results reveal that thickness of the sika wrap strip significantly increases the edge peeling and shear stresses. Generally, the thickness of sika wrap plate used in practical engineering is very small, compared with that of other plate. It is shown that the level and concentration of interfacial stress are influenced considerably by the thickness of the sika wrap plate. Therefore, the fact of the smaller interfacial stress level and concentration should be one of the advantages of retrofitting by sika wrap.

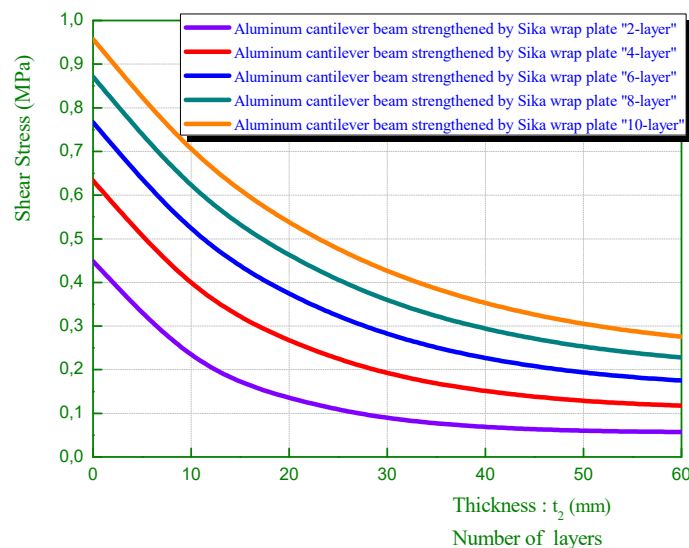


Fig. 5 Effect of plate stiffness “number of layers” on interfacial shear stresses in strengthened aluminum cantilever beam

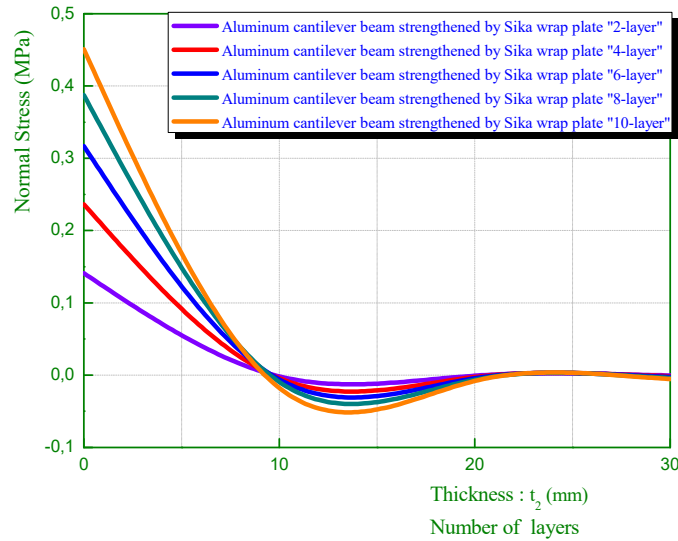


Fig. 6 Effect of plate stiffness “number of layers” on interfacial normal stresses in strengthened aluminum cantilever beam

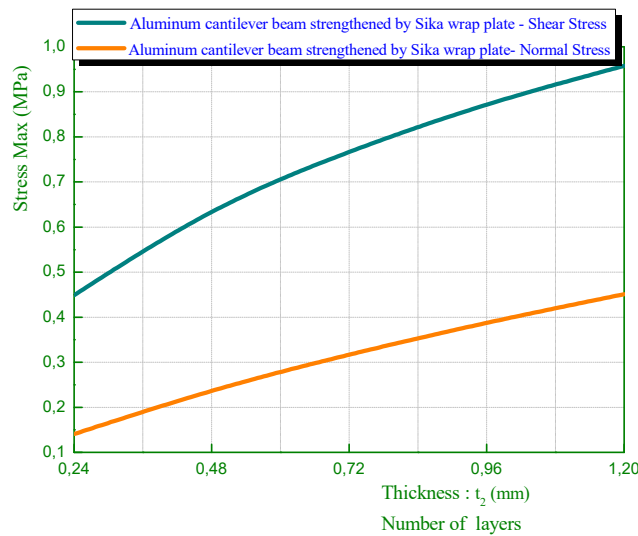


Fig. 7 Effect of thickness plate on interfacial stresses in strengthened aluminum cantilever beam

### 3.6 Effect on plate length of the strengthened cantilever beam region $L_p$

The influence of length of the strengthened beam region  $L_p$  appears in Fig. 8. It is seen that, as the plate terminates further away from the supports, the interfacial stresses increase significantly. This result reveals that in any case of strengthening, including cases where retrofitting is required in a limited zone of maximum bending moments, it is recommended to extend the strengthening strip as close as possible to the free end of the cantilever beam.

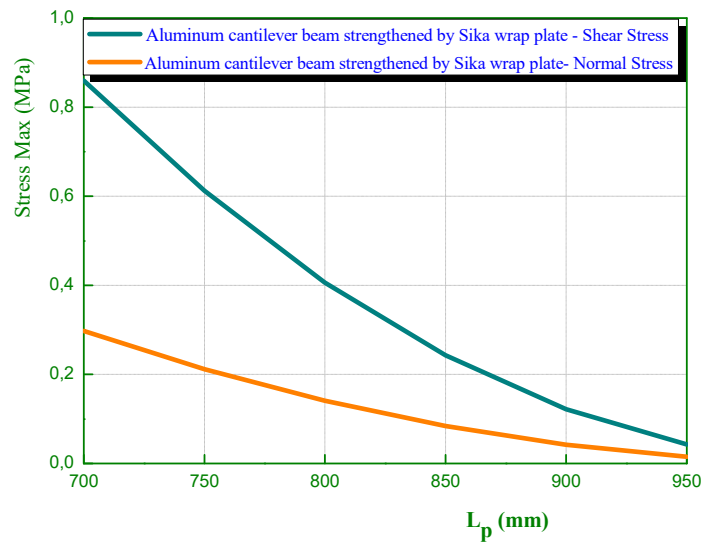


Fig. 8 Effect of plate length on edge stresses interfacial stresses in strengthened aluminum cantilever beam

### 3.7 Effect of elasticity modulus of adhesive layer

The adhesive layer is a relatively soft, isotropic material and has a smaller stiffness. The four sets of Young’s moduli are considered here, which are 3, 4, 5 and 6.7 GPa. The Poisson’s ratio of the adhesive is kept constant. The numerical results in Figs. 9, 10 and 11 show that the property of the adhesive hardly influences the level of the interfacial stresses, whether normal or shear stress, but the stress concentrations at the end of the plate increase as the Young’s modulus of the adhesive increases.

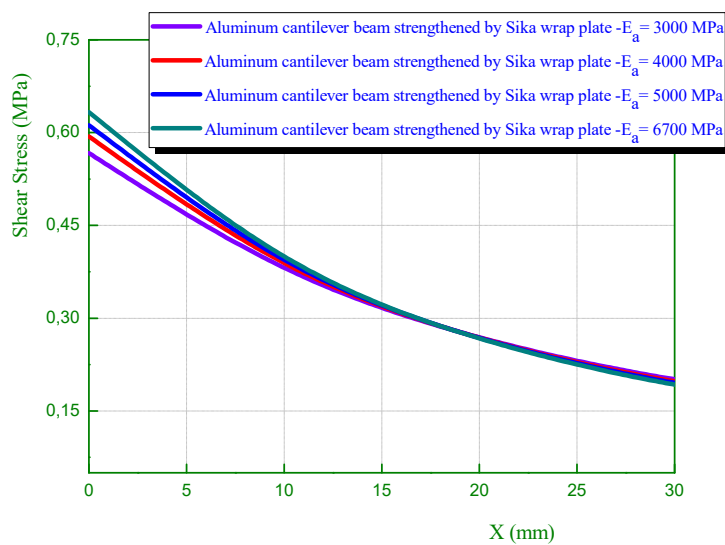


Fig. 9 Effect of adhesive moduli on interfacial shear stresses in strengthened aluminum cantilever beam

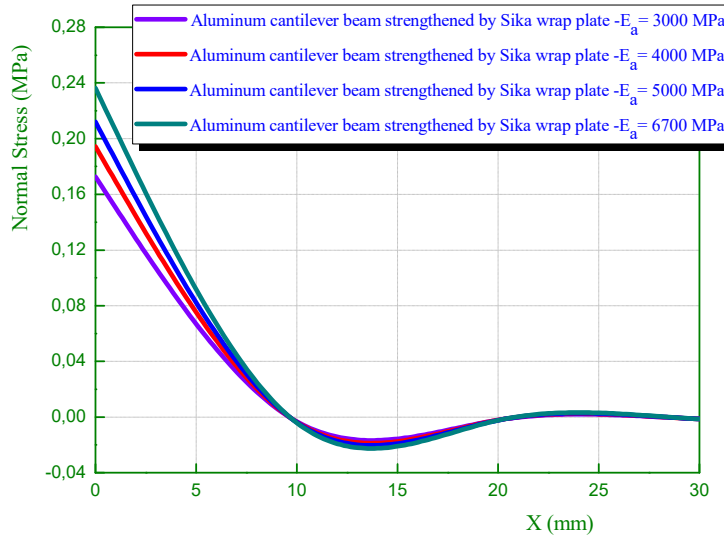


Fig. 10 Effect of adhesive moduli on interfacial normal stresses in strengthened aluminum cantilever beam

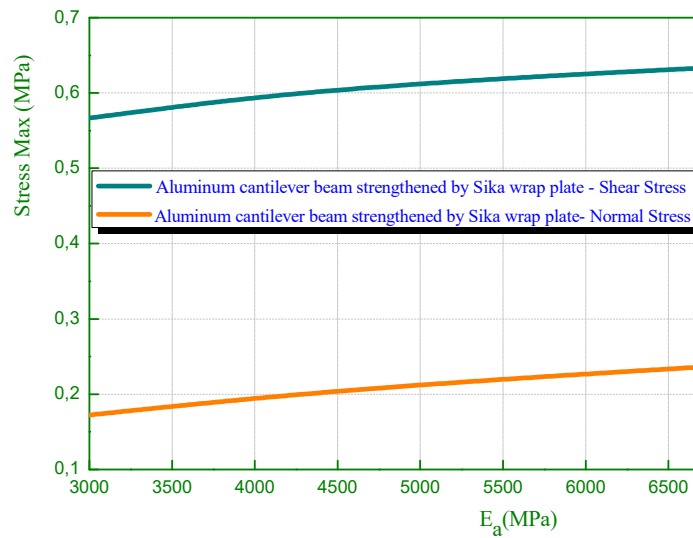


Fig. 11 Effect of adhesive moduli on interfacial stresses in strengthened aluminum cantilever beam

### 3.8 Effect of the adhesive layer thickness

Fig. 12 shows the effects of the thickness of the adhesive layer on the interfacial stresses. It is seen that increasing the thickness of the adhesive layer leads to significant reduction in the peak interfacial stresses. Thus, using thick adhesive layer, especially in the vicinity of the edge, is recommended.

This paper has been concerned with the prediction of interfacial shear and normal stresses in aluminum cantilever beams retrofitted with externally advanced composite materials. Such interfacial stresses provide the basis for understanding debonding failures in such beams and for



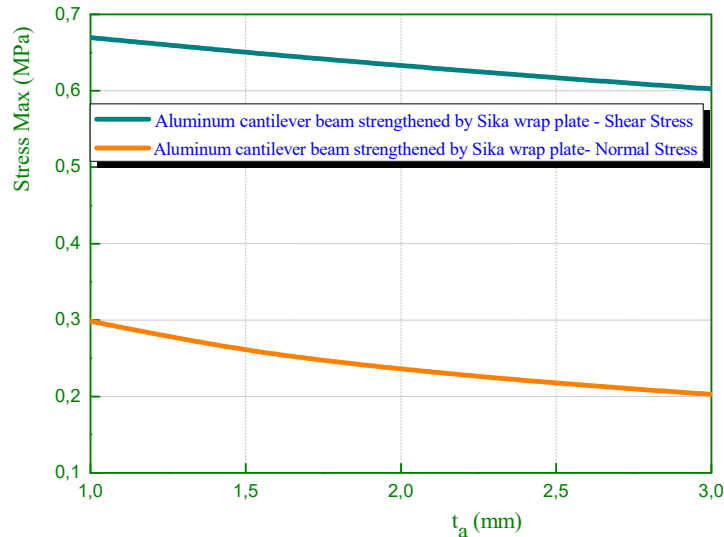


Fig. 12 Effect of adhesive layer thickness on interfacial stresses in strengthened aluminum cantilever beam

development of suitable design rules. The adherend shear deformations have been included in the theoretical analyses by assuming linear shear stress distributions through the thickness of the adherends, the classical solutions which neglect the adherend shear deformations over-estimate the non-uniformity of the adhesive stresses distributions and maximum interfacial stresses. Numerical comparison between the existing solutions and the present new solution has been carried out. In the final part of this paper, extensive parametric studies were undertaken by using the new solution for strengthened beams with various ratios of design parameters. Observations were made based on the numerical results concerning their possible implications to practical designs. On the basis of the results obtained from the new model, we can say that the new solution is general in nature and may be applicable to all kinds of materials.

In conclusion, we can say that in addition to matrix composite fiber materials, another alternative may be proposed for strengthening aluminum structures, this will involve the use of functionally graded materials FGM (Tounsi *et al.* 2020, Zaoui *et al.* 2019, Zine *et al.* 2020, Hadj *et al.* 2019, Chaabane *et al.* 2019, Chikr *et al.* 2020, Daouadji and Benferhat 2016, Kaddari *et al.* 2020, Benferhat *et al.* 2016b, Adim and Daouadji 2016 and Benhenni *et al.* 2018) in order to ensure continuity properties lift through the thickness of the reinforcement plate.

#### 4. Conclusions

This research was supported by the Algerian Ministry of Higher Education and Scientific Research (MESRS) as part of the grant for the PRFU research project n° A01L02UN140120200002 and by the University of Tiaret, in Algeria.

#### References

Abderezak, R., Daouadji, T.H., Rabia, B. and Belkacem, A. (2016), "Analysis of buckling response of

- functionally graded sandwich plates using a refined shear deformation theory”, *Wind Struct., Int. J.*, **22**(3), 291-305. <https://doi.org/10.12989/was.2016.22.3.291>
- Abderezak, R., Daouadji, T.H., Rabia, B. and Belkacem, A. (2018), “Nonlinear analysis of damaged RC beams strengthened with glass fiber reinforced polymer plate under symmetric loads”, *Earthq. Struct., Int. J.*, **15**(1), 113-122. <https://doi.org/10.12989/eas.2018.15.2.113>
- Abderezak, R., Rabia, B., Daouadji, T.H., Abbes, B., Belkacem, A. and Abbes, F. (2019), “Elastic analysis of interfacial stresses in prestressed PFGM-RC hybrid beams”, *Adv. Mater. Res., Int. J.*, **7**(2), 83-103. <https://doi.org/10.12989/amr.2018.7.2.083>
- Abderezak, R., Daouadji, T.H. and Rabia, B. (2020), “Analysis of interfacial stresses of the reinforced concrete foundation beams repairing with composite materials plate”, *Coupl. Syst. Mech., Int. J.*, **9**(5), 473-498. <http://doi.org/10.12989/csm.2020.9.5.473>
- Abdelouahed, A. (2006), “Improved theoretical solution for interfacial stresses in concrete beams strengthened with FRP plate”, *Int. J. Solids Struct.*, **43**(14-15), 4154-4174. <https://doi.org/10.1016/j.ijsolstr.2005.03.074>
- Abualnour, M., Houari, M.S.A., Tounsi, A. and Mahmoud, S.R. (2018), “A novel quasi-3D trigonometric plate theory for free vibration analysis of advanced composite plates”, *Compos. Struct.*, **184**, 688-697. <https://doi.org/10.1016/j.compstruct.2017.10.047>
- Addou, F.Y., Meradjah, M., Bousahla, A.A., Benachour, A., Bourada, F., Tounsi, A. and Mahmoud, S.R. (2019), “Influences of porosity on dynamic response of FG plates resting on Winkler/Pasternak/Kerr foundation using quasi 3D HSDT”, *Comput. Concrete, Int. J.*, **24**(4), 347-367. <https://doi.org/10.12989/cac.2019.24.4.347>
- Adim, B. and Daouadji, T.H. (2016), “Effects of thickness stretching in FGM plates using a quasi-3D higher order shear deformation theory”, *Adv. Mater. Res., Int. J.*, **5**(4), 223-244. <https://doi.org/10.12989/amr.2016.5.4.223>
- Al-Furjan, M.S.H., Safarpour, H., Habibi, M., Safarpour, M. and Tounsi, A. (2020a), “A comprehensive computational approach for nonlinear thermal instability of the electrically FG-GPLRC disk based on GDQ method”, *Eng. Comput.* <https://doi.org/10.1007/s00366-020-01088-7>
- Al-Furjan, M.S.H., Habibi, M., Chen, G., Safarpour, H., Safarpour, M. and Tounsi, A. (2020b), “Chaotic oscillation of a multi-scale hybrid nano-composites reinforced disk under harmonic excitation via GDQM”, *Compos. Struct.*, **252**, 112737. <https://doi.org/10.1016/j.compstruct.2020.112737>
- Alimirzaei, S., Mohammadimehr, M. and Tounsi, A. (2019), “Nonlinear analysis of viscoelastic micro-composite beam with geometrical imperfection using FEM: MSGT electro-magneto-elastic bending, buckling and vibration solutions”, *Struct. Eng. Mech., Int. J.*, **71**(5), 485-502. <https://doi.org/10.12989/sem.2019.71.5.485>
- Antar, K., Amara, K., Benyoucef, S., Bouazza, M. and Ellali, M. (2019), “Hygrothermal effects on the behavior of reinforced-concrete beams strengthened by bonded composite laminate plates”, *Struct. Eng. Mech., Int. J.*, **69**(3), 327-334. <https://doi.org/10.12989/sem.2019.69.3.327>
- Balubaid, M., Tounsi, A., Dakhel, B. and Mahmoud, S.R. (2019), “Free vibration investigation of FG nanoscale plate using nonlocal two variables integral refined plate theory”, *Comput. Concrete, Int. J.*, **24**(6), 579-586. <https://doi.org/10.12989/cac.2019.24.6.579>
- Belabed, Z., Bousahla, A.A., Houari, M.S.A., Tounsi, A. and Mahmoud, S.R. (2018), “A new 3-unknown hyperbolic shear deformation theory for vibration of functionally graded sandwich plate”, *Earthq. Struct., Int. J.*, **14**(2), 103-115. <https://doi.org/10.12989/eas.2018.14.2.103>
- Belkacem, A., Tahar, H.D., Abderrezak, R., Amine, B.M., Mohamed, Z. and Boussad, A. (2018), “Mechanical buckling analysis of hybrid laminated composite plates under different boundary conditions”, *Struct. Eng. Mech., Int. J.*, **66**(6), 761-769. <https://doi.org/10.12989/sem.2018.66.6.761>
- Bellal, M., Hebali, H., Heireche, H., Bousahla, A.A., Tounsi, A., Bourada, F., Mahmoud, S.R., Bedia, E.A. and Tounsi, A. (2020), “Buckling behavior of a single-layered graphene sheet resting on viscoelastic medium via nonlocal four-unknown integral model”, *Steel Compos. Struct., Int. J.*, **34**(5), 643-655. <https://doi.org/10.12989/scs.2020.34.5.643>
- Benachour, A., Benyoucef, S. and Tounsi, A. (2008), “Interfacial stress analysis of steel beams reinforced with bonded prestressed FRP plate”, *Eng. Struct.*, **30**, 3305-3315.

- <https://doi.org/10.1016/j.engstruct.2008.05.007>
- Benferhat, R., Hassaine Daouadji, T., Hadji, L. and Said Mansour, M. (2016a), "Static analysis of the FGM plate with porosities", *Steel Compos. Struct., Int. J.*, **21**(1), 123-136.  
<https://doi.org/10.12989/scs.2016.21.1.123>
- Benferhat, R., Daouadji, T.H., Mansour, M.S. and Hadji, L. (2016b), "Effect of porosity on the bending and free vibration response of functionally graded plates resting on Winkler-Pasternak foundations", *Eartq. Struct., Int. J.*, **10**(5), 1429-1449. <https://doi.org/10.12989/eas.2016.10.5.1033>
- Benferhat, R., Hassaine Daouadji, T., Hadji, L. and Said Mansour, M. (2016c), "Static analysis of the FGM plate with porosities", *Steel Compos. Struct., Int. J.*, **21**(1), 123-136.  
<https://doi.org/10.12989/scs.2016.21.1.123>
- Benhenni, M.A., Daouadji, T.H., Abbes, B., Adim, B., Li, Y. and Abbes, F. (2018), "Dynamic analysis for anti-symmetric cross-ply and angle-ply laminates for simply supported thick hybrid rectangular plates", *Adv. Mater. Res., Int. J.*, **7**(2), 83-103. <https://doi.org/10.12989/amr.2018.7.2.119>
- Benhenni, M.A., Daouadji, T.H., Abbes, B., Abbes, F., Li, Y. and Adim, B. (2019a), "Numerical analysis for free vibration of hybrid laminated composite plates for different boundary conditions", *Struct. Eng. Mech., Int. J.*, **70**(5), 535-549. <https://doi.org/10.12989/sem.2019.70.5.535>
- Benhenni, M.A., Adim, B., Daouadji, T.H., Abbès, B., Abbès, F., Li, Y. and Bouzidane, A. (2019b), "A comparison of closed form and finite element solutions for the free vibration of hybrid cross ply laminated plates", *Mech. Compos. Mater.*, **55**(2), 181-194. <https://doi.org/10.1007/s11029-019-09803-2>
- Bensattalah, T., Daouadji, T.H., Zidour, M., Tounsi, A. and Bedia, E.A. (2016), "Investigation of thermal and chirality effects on vibration of single walled carbon nanotubes embedded in a polymeric matrix using nonlocal elasticity theories", *Mech. Compos. Mater.*, **52**(4), 555-568.  
<https://doi.org/10.1007/s11029-016-9606-z>
- Bensattalah, T., Zidour, M. and Daouadji, T.H. (2018), "Analytical analysis for the forced vibration of CNT surrounding elastic medium including thermal effect using nonlocal Euler-Bernoulli theory", *Adv. Mater. Res., Int. J.*, **7**(3), 163-174. <https://doi.org/10.12989/amr.2018.7.3.163>
- Berghouti, H., Adda Bedia, E.A., Benkhedda, A. and Tounsi, A. (2019), "Vibration analysis of nonlocal porous nanobeams made of functionally graded material", *Adv. Nano Res., Int. J.*, **7**(5), 351-364.  
<https://doi.org/10.12989/anr.2019.7.5.351>
- Bouakaz, K., Daouadji, T.H., Meftah, S.A., Ameer, M., Tounsi, A. and Bedia, E.A. (2014), "A Numerical analysis of steel beams strengthened with composite materials", *Mech. Compos. Mater.*, **50**(4), 685-696.  
<https://doi.org/10.1007/s11029-014-9435-x>
- Boukhlif, Z., Bouremana, M., Bourada, F., Bousahla, A.A., Bourada, M., Tounsi, A. and Al-Osta, M.A. (2019), "A simple quasi-3D HSDT for the dynamics analysis of FG thick plate on elastic foundation", *Steel Compos. Struct., Int. J.*, **31**(5), 503-516. <https://doi.org/10.12989/scs.2019.31.5.503>
- Boulefrakh, L., Hebali, H., Chikh, A., Bousahla, A.A., Tounsi, A. and Mahmoud, S.R. (2019), "The effect of parameters of visco-Pasternak foundation on the bending and vibration properties of a thick FG plate", *Geomech. Eng., Int. J.*, **18**(2), 161-178. <https://doi.org/10.12989/gae.2019.18.2.161>
- Bourada, F., Bousahla, A.A., Bourada, M., Azzaz, A., Zinata, A. and Tounsi, A. (2019), "Dynamic investigation of porous functionally graded beam using a sinusoidal shear deformation theory", *Wind Struct., Int. J.*, **28**(1), 19-30. <https://doi.org/10.12989/was.2019.28.1.019>
- Bourada, F., Bousahla, A.A., Tounsi, A., Bedia, E.A., Mahmoud, S.R., Benrahou, K.H. and Tounsi, A. (2020), "Stability and dynamic analyses of SW-CNT reinforced concrete beam resting on elastic-foundation", *Comput. Concrete, Int. J.*, **25**(6), 485-495. <https://doi.org/10.12989/cac.2020.25.6.485>
- Bousahla, A.A., Bourada, F., Mahmoud, S.R., Tounsi, A., Algarni, A., Bedia, E.A. and Tounsi, A. (2020), "Buckling and dynamic behavior of the simply supported CNT-RC beams using an integral-first shear deformation theory", *Comput. Concrete, Int. J.*, **25**(2), 155-166. <https://doi.org/10.12989/cac.2020.25.2.155>
- Chaabane, L.A., Bourada, F., Sekkal, M., Zerouati, S., Zaoui, F.Z., Tounsi, A., Derras, A., Bousahla, A.A. and Tounsi, A. (2019), "Analytical study of bending and free vibration responses of functionally graded beams resting on elastic foundation", *Struct. Eng. Mech., Int. J.*, **71**(2), 185-196.  
<https://doi.org/10.12989/sem.2019.71.2.185>

- Chedad, A., Daouadji, T.H., Abderezak, R., Belkacem, A., Abbes, B., Rabia, B. and Abbes, F. (2018), "A high-order closed-form solution for interfacial stresses in externally sandwich FGM plated RC beams", *Adv. Mater. Res., Int. J.*, **6**(4), 317-328. <https://doi.org/10.12989/amr.2017.6.4.317>
- Chergui, S., Daouadji, T.H., Hamrat, M., Boulekbache, B., Bougara, A., Abbes, B. and Amziane, S. (2019), "Interfacial stresses in damaged RC beams strengthened by externally bonded prestressed GFRP laminate plate: Analytical and numerical study", *Adv. Mater. Res., Int. J.*, **8**(3), 197-217. <https://doi.org/10.12989/amr.2019.8.3.197>
- Chikr, S.C., Kaci, A., Bousahla, A.A., Bourada, F., Tounsi, A., Bedia, E.A., Mahmoud, S.R., Benrahou, K.H. and Tounsi, A. (2020), "A novel four-unknown integral model for buckling response of FG sandwich plates resting on elastic foundations under various boundary conditions using Galerkin's approach", *Geomech. Eng., Int. J.*, **21**(5), 471-487. <https://doi.org/10.12989/gae.2020.21.5.471>
- Daouadji, T.H. (2013), "Analytical analysis of the interfacial stress in damaged reinforced concrete beams strengthened by bonded composite plates", *Strength Mater.*, **45**(5), 587-597. <https://doi.org/10.1007/s11223-013-9496-4>
- Daouadji, T.H. (2016), "Theoretical analysis of composite beams under uniformly distributed load", *Adv. Mater. Res., Int. J.*, **5**(1), 1-9. <https://doi.org/10.12989/amr.2016.5.1.001>
- Daouadji, T.H. (2017), "Analytical and numerical modeling of interfacial stresses in beams bonded with a thin plate", *Adv. Computat. Des., Int. J.*, **2**(1), 57-69. <https://doi.org/10.12989/acd.2017.2.1.057>
- Daouadji, T.H. and Adim, B. (2016a), "An analytical approach for buckling of functionally graded plates", *Adv. Mater. Res., Int. J.*, **5**(3), 141-169. <https://doi.org/10.12989/amr.2016.5.3.141>
- Daouadji, T.H. and Benferhat, R. (2016), "Bending analysis of an imperfect FGM plates under hygro-thermo-mechanical loading with analytical validation", *Adv. Mater. Res., Int. J.*, **5**(1), 35-53. <https://doi.org/10.12989/amr.2016.5.1.035>
- Daouadji, T.H. and Benferhat, R. (2016), "Bending analysis of an imperfect FGM plates under hygro-thermo-mechanical loading with analytical validation", *Adv. Mater. Res., Int. J.*, **5**(1), 35-53. <https://doi.org/10.12989/amr.2016.5.1.035>
- Guenaneche, B. and Tounsi, A. (2014), "Effect of shear deformation on interfacial stress analysis in plated beams under arbitrary loading", *Adhes. Adhes.*, **48**, 1-13. <https://doi.org/10.1016/j.ijadhadh.2013.09.016>
- Hadj, B., Rabia, B. and Daouadji, T.H. (2019), "Influence of the distribution shape of porosity on the bending FGM new plate model resting on elastic foundations", *Struct. Eng. Mech., Int. J.*, **72**(1), 823-832. <https://doi.org/10.12989/sem.2019.72.1.061>
- Hamrat, M., Bouziadi, F., Boulekbache, B., Daouadji, T.H., Chergui, S., Labed, A. and Amziane, S. (2020), "Experimental and numerical investigation on the deflection behavior of pre-cracked and repaired reinforced concrete beams with fiber-reinforced polymer", *Constr. Build. Mater.*, **249**, 118745. <https://doi.org/10.1016/j.conbuildmat.2020.118745>
- He, X.J., Zhou, C.Y. and Wang, Y. (2019), "Interfacial stresses in reinforced concrete cantilever members strengthened with fibre-reinforced polymer laminates", *Adv. Struct. Eng.*, 1-12. <https://doi.org/10.1177/1369433219868933>
- Kaddari, M., Kaci, A., Bousahla, A.A., Tounsi, A., Bourada, F., Tounsi, A., Bedia, E.A. and Al-Osta, M.A. (2020), "A study on the structural behaviour of functionally graded porous plates on elastic foundation using a new quasi-3D model: Bending and Free vibration analysis", *Comput. Concrete, Int. J.*, **25**(1), 37-57. <https://doi.org/10.12989/cac.2020.25.1.037>
- Khelifa, Z., Hadji, L., Daouadji, T.H. and Bourada, M. (2018), "Buckling response with stretching effect of carbon nanotube-reinforced composite beams resting on elastic foundation", *Struct. Eng. Mech., Int. J.*, **67**(2), 125-130. <https://doi.org/10.12989/sem.2018.67.2.125>
- Larrinaga, P., Garmendia, L., Piñero, I. and San-José, J.T. (2020), "Flexural strengthening of low-grade reinforced concrete beams with compatible composite material: Steel Reinforced Grout (SRG)", *Constr. Build. Mater.*, **235**, 117790. <https://doi.org/10.1016/j.conbuildmat.2019.117790>
- Liu, S., Zhou, Y., Zheng, Q., Zhou, J., Jin, F. and Fan, H. (2019), "Blast responses of concrete beams reinforced with steel-GFRP composite bars", *Structures*, **22**, 200-212. <https://doi.org/10.1016/j.istruc.2019.08.010>

- Matouk, H., Bousahla, A.A., Heireche, H., Bourada, F., Bedia, E.A., Tounsi, A., Mahmoud, S.R., Tounsi, A. and Benrahou, K.H. (2020), "Investigation on hygro-thermal vibration of P-FG and symmetricS-FG nanobeam using integral Timoshenko beam theory", *Adv. Nano Res., Int. J.*, **8**(4), 293-305. <https://doi.org/10.12989/anr.2020.8.4.293>
- Menasria, A., Kaci, A., Bousahla, A.A., Bourada, F., Tounsi, A., Benrahou, K.H., Tounsi, A., Adda Bedia, E.A. and Mahmoud, S.R. (2020), "A four-unknown refined plate theory for dynamic analysis of FG-sandwich plates under various boundary conditions", *Steel Compos. Struct., Int. J.*, **36**(3), 355-367. <https://doi.org/10.12989/scs.2020.36.3.355>
- Mokhtar, Y., Heireche, H., Bousahla, A.A., Houari, M.S.A., Tounsi, A. and Mahmoud, S.R. (2018), "A novel shear deformation theory for buckling analysis of single layer graphene sheet based on nonlocal elasticity theory", *Smart Struct. Syst., Int. J.*, **21**(4), 397-405. <https://doi.org/10.12989/sss.2018.21.4.397>
- Panjehpour, M., Farzadnia, N., Demirboga, R. and Ali, A.A.A. (2016), "Behavior of high-strength concrete cylinders repaired with CFRP sheets", *J. Civil Eng. Manag.*, **22**(1), 56-64. <https://doi.org/10.3846/13923730.2014.897965>
- Rabahi, A., Daouadji, T.H., Abbes, B. and Adim, B. (2016), "Analytical and numerical solution of the interfacial stress in reinforced-concrete beams reinforced with bonded prestressed composite plate", *J. Reinf. Plast. Compos.*, **35**(3), 258-272. <https://doi.org/10.1177/0731684415613633>
- Rabhi, M., Benrahou, K.H., Kaci, A., Houari, M.S.A., Bourada, F., Bousahla, A.A., Tounsi, A., Adda Bedia, E.A., Mahmoud, S.R. and Tounsi, A. (2020), "A new innovative 3-unknowns HSDT for buckling and free vibration of exponentially graded sandwich plates resting on elastic foundations under various boundary conditions", *Geomech. Eng., Int. J.*, **22**(2), 119-132. <https://doi.org/10.12989/gae.2020.22.2.119>
- Rabia, B., Abderezak, R., Daouadji, T.H., Abbes, B., Belkacem, A. and Abbes, F. (2018), "Analytical analysis of the interfacial shear stress in RC beams strengthened with prestressed exponentially-varying properties plate", *Adv. Mater. Res., Int. J.*, **7**(1), 29-44. <https://doi.org/10.12989/amr.2018.7.1.029>
- Rabia, B., Daouadji, T.H. and Abderezak, R. (2019), "Effect of distribution shape of the porosity on the interfacial stresses of the FGM beam strengthened with FRP plate", *Earthq. Struct., Int. J.*, **16**(5), 601-609. <https://doi.org/10.12989/eas.2019.16.5.601>
- Refrafi, S., Bousahla, A.A., Bouhadra, A., Menasria, A., Bourada, F., Tounsi, A., Bedia, E.A., Mahmoud, S.R., Benrahou, K.H. and Tounsi, A. (2020), "Effects of hygro-thermo-mechanical conditions on the buckling of FG sandwich plates resting on elastic foundations", *Comput. Concrete, Int. J.*, **25**(4), 311-325. <https://doi.org/10.12989/cac.2020.25.4.311>
- Rahmani, M.C., Kaci, A., Bousahla, A.A., Bourada, F., Tounsi, A., Bedia, E.A., Mahmoud, S.R., Benrahou, K.H. and Tounsi, A. (2020), "Influence of boundary conditions on the bending and free vibration behavior of FGM sandwich plates using a four-unknown refined integral plate theory", *Comput. Concrete, Int. J.*, **25**(3), 225-244. <https://doi.org/10.12989/cac.2020.25.3.225>
- Sahla, M., Saidi, H., Draiche, K., Bousahla, A.A., Bourada, F. and Tounsi, A. (2019), "Free vibration analysis of angle-ply laminated composite and soft core sandwich plates", *Steel Compos. Struct., Int. J.*, **33**(5), 663-679. <https://doi.org/10.12989/scs.2019.33.5.663>
- Shariati, A., Ghabussi, A., Habibi, M., Safarpour, H., Safarpour, M., Tounsi, A. and Safa, M. (2020), "Extremely large oscillation and nonlinear frequency of a multi-scale hybrid disk resting on nonlinear elastic foundations", *Thin-Wall. Struct.*, **154**, 106840. <https://doi.org/10.1016/j.tws.2020.106840>
- Smith, S.T. and Teng, J.G. (2002), "Interfacial stresses in plated beams", *Eng. Struct.*, **23**(7), 857-871. [https://doi.org/10.1016/S0141-0296\(00\)00090-0](https://doi.org/10.1016/S0141-0296(00)00090-0)
- Tahar, H.D., Boussad, A., Abderezak, R., Rabia, B., Fazilay, A. and Belkacem, A. (2019), "Flexural behaviour of steel beams reinforced by carbon fibre reinforced polymer: Experimental and numerical study", *Struct. Eng. Mech., Int. J.*, **72**(4), 409-419. <https://doi.org/10.12989/sem.2019.72.4.409>
- Tahar, H.D., Abderezak, R. and Rabia, B. (2020), "Flexural performance of wooden beams strengthened by composite plate", *Struct. Monitor. Maint., Int. J.*, **7**(3), 233-259. <https://doi.org/10.12989/smm.2020.7.3.233>
- Tayeb, B. and Daouadji, T.H. (2020), "Improved analytical solution for slip and interfacial stress in composite steel-concrete beam bonded with an adhesive", *Adv. Mater. Res., Int. J.*, **9**(2), 133-153.

- <https://doi.org/10.12989/amr.2020.9.2.133>
- Tayeb, T.S., Zidour, M., Bensattalah, T., Heireche, H., Benahmed, A. and Bedia, E.A. (2020), "Mechanical buckling of FG-CNTs reinforced composite plate with parabolic distribution using Hamilton's energy principle", *Adv. Nano Res., Int. J.*, **8**(2), 135-148. <https://doi.org/10.12989/anr.2020.8.2.135>
- Tounsi, A., Daouadji, T.H. and Benyoucef, S. (2008), "Interfacial stresses in FRP-plated RC beams: Effect of adherend shear deformations", *Int. J. Adhes. Adhes.*, **29**, 313-351. <https://doi.org/10.1016/j.ijadhadh.2008.06.008>
- Tounsi, A., Houari, M.S.A. and Benyoucef, S. (2013), "A refined trigonometric shear deformation theory for thermoelastic bending of functionally graded sandwich plates", *Aerosp. Sci. Technol.*, **24**, 209-220. <https://doi.org/10.1016/j.ast.2011.11.009>
- Tounsi, A., Al-Dulajjan, S.U., Al-Osta, M.A., Chikh, A., Al-Zahrani, M.M., Sharif, A. and Tounsi, A. (2020), "A four variable trigonometric integral plate theory for hygro-thermo-mechanical bending analysis of AFG ceramic-metal plates resting on a two-parameter elastic foundation", *Steel Compos. Struct., Int. J.*, **34**(4), 511-524. <https://doi.org/10.12989/scs.2020.34.4.511>
- Wang, Y.H., Yu, J., Liu, J.P., Zhou, B.X. and Chen, Y.F. (2020), "Experimental study on assembled monolithic steel-prestressed concrete composite beam in negative moment", *J. Constr. Steel Res.*, **167**, 105667. <https://doi.org/10.1016/j.jcsr.2019.06.004>
- Yuan, C., Chen, W., Pham, T.M. and Hao, H. (2019), "Effect of aggregate size on bond behaviour between basalt fibre reinforced polymer sheets and concrete", *Compos. Part B: Eng.*, **158**, 459-474. <https://doi.org/10.1016/j.compositesb.2018.09.089>
- Zaoui, F.Z., Ouinas, D. and Tounsi, A. (2019), "New 2D and quasi-3D shear deformation theories for free vibration of functionally graded plates on elastic foundations", *Compos. Part B*, **159**, 231-247. <https://doi.org/10.1016/j.compositesb.2018.09.051>
- Zine, A., Bousahla, A.A., Bourada, F., Benrahou, K.H., Tounsi, A., Adda Bedia, E.A., Mahmoud, S.R. and Tounsi, A. (2020), "Bending analysis of functionally graded porous plates via a refined shear deformation theory", *Comput. Concrete, Int. J.*, **26**(1), 63-74. <https://doi.org/10.12989/cac.2020.26.1.063>